Neurochemical Research (2019) 44:228–233
https://doi.org/10.1007/s11064-017-2461-z

ORIGINAL PAPER

Impaired Cu–Zn Superoxide Dismutase (SOD1) and Calcineurin (Cn) Interaction in ALS: A Presumed Consequence for TDP-43 and Zinc Aggregation in Tg SOD1^{G93A} Rodent Spinal Cord Tissue

Jolene M. Kim[1] · Elizabeth Billington[1] · Ada Reyes[1] · Tara Notarianni[1] · Jessica Sage[1] · Emre Agbas[2] · Michael Taylor[1] · Ian Monast[1] · John A. Stanford[3] · Abdulbaki Agbas[1]

Received: 15 November 2017 / Accepted: 26 December 2017 / Published online: 3 January 2018

Abstract

Impaired interactions between Calcineurin (Cn) and (Cu/Zn) superoxide dismutase (SOD1) are suspected to be responsible for the formation of hyperphosphorylated protein aggregation in amyotrophic lateral sclerosis (ALS). Serine (Ser)- enriched phosphorylated TDP-43 protein aggregation appears in the spinal cord of ALS animal models, and may be linked to the reduced phosphatase activity of Cn. The mutant overexpressed SOD1^{G93A} protein does not properly bind zinc (Zn) in animal models; hence, mutant SOD1^{G93A}–Cn interaction weakens. Consequently, unstable Cn fails to dephosphorylate TDP-43 that yields hyperphosphorylated TDP-43 aggregates. Our previous studies had suggested that Cn and SOD1 interaction was necessary to keep Cn enzyme functional. We have observed low Cn level, increased Zn concentrations, and increased TDP-43 protein levels in cervical, thoracic, lumbar, and sacral regions of the spinal cord tissue homogenates. This study further supports our previously published work indicating that Cn stability depends on functional Cn–SOD1 interaction because Zn is crucial for maintaining the Cn stability. Less active Cn did not efficiently dephosphorylate TDP-43; hence TDP-43 aggregations appeared in the spinal cord tissue.

Keywords ALS · TDP-43 · SOD1^{G93A} · Calcineurin · Spinal cord

Introduction

Amyotrophic lateral sclerosis (ALS) (a.k.a. Lou Gehrig Disease) is a non-treatable progressive neurodegenerative disease that is 100% fatal and claims about 30,000 lives per year in the USA (http://www.als.org). Nearly 90% of these cases are sporadic. The disease is characterized by the selective loss of motor neurons in the spinal cord, brain stem, and cerebral (motor) cortex [1]. The causative factors of the disease remain contentious at a molecular level, although the hallmark of ALS is the formation of superoxide dismutase-enriched plaques in Lewy bodies in the spinal cord [2]. Involvement of a previously discovered protein TDP-43 in ALS pathogenesis [3, 4] has recently attracted attention, resulting in several important papers published during the last decade [5–10]. Trans activating response region DNA binding protein (TDP-43)-enriched plaques are observed in ALS, and TDP-43 mutation-induced aggregates are considered as a promoting factor in ALS pathology [11]. TDP-43 phosphorylation and subsequent aggregation have been found in motor neurons [12, 13], suggesting that TDP-43

Jolene M. Kim, Elizabeth Billington have contributed equally to this work.

Electronic supplementary material The online version of this article (https://doi.org/10.1007/s11064-017-2461-z) contains supplementary material, which is available to authorized users.

✉ Abdulbaki Agbas
aagbas@kcumb.edu

[1] Division of Basic Sciences, College of Osteopathic Medicine, Kansas City University of Medicine and Biosciences, 1750 Independence Avenue, Kansas City, MO 6410, USA

[2] Stowers Institute for Medical Research, 1000 E 50th Street, Kansas City, MO 64110, USA

[3] University of Kansas Medical Center, 3901 Rainbow Blvd., 2096 HLSIC, Kansas City, KS 66160, USA

aggregation due to abnormal phosphorylation may also be relevant to reduced activity of Cn in ALS, since phosphatase Cn regulates the TDP-43 phosphorylation in both lower and higher organisms [14].

Partial inactivation of Cn in both sporadic and familial ALS patients as well as in an asymptomatic carrier of a dominant SOD1 mutation may suggest the role of Cn in the pathogenesis of ALS [15].Both Cn and SOD1 are zinc (Zn)-containing metalloproteins [16–21]. The failure of this protein–protein interaction(s) may lead to increased labile Zn accumulation, thereby causing toxicity in motor neurons [22, 23]. Therefore, the involvement of Zn in the development of ALS is another critical concept to be considered since metal cations and oxidative injury have been implicated in the pathogenesis of ALS [24, 25].

Elucidating these multiple factors will contribute to a basic understanding of Cn/SOD1/TDP-43 protein interactions that may occur in the early stages of ALS development. This could lead to early treatment options focused on restoring normal protein–protein interactions [26].

The focus of our work is to provide some preliminary evidence that reduced Cn activity is due to weakened interactions between SOD1 and Cn in the transgenic (Tg) $SOD1^{G93A}$ rodent (i.e., rat and mouse) model. We hypothesize that poorly bound Zn in both metallo-enzymes (i.e. SOD1 and Cn) dissociate and accumulate in the cytosol, eventually inducing motor neuron death [27]. Subsequently, the less functional Cn enzyme would fail to dephosphorylate TDP-43, leading to the formation of hyperphosphorylated TDP-43 aggregates that are considered to be the hallmark of neuropathology in 90% of ALS cases [12].

Materials and Methods

Animals

Tg $SOD1^{G93A}$ rat (B6.Cg-Tg(SOD1*G93A)1Gur/J) breeders were obtained from Taconic and offspring were genotyped using the protocol described in the Jackson Laboratory website (https://www2.jax.org/protocolsdb/f?p=116:5:0::NO:5:P5_MASTER_PROTOCOL_ID,P5_JRS_CODE:9877,004435). Rats were fed normal chow (Harlan Teklad rodent diet 8604 from Teklad diets, Madison, WI) and were housed in University of Kansas Medical Center (KUMC) animal facilities for 6 months. Animal use was approved by KUMC IACUC protocol (#2013-2142).

Tissues

After animals were deeply anesthetized and decapitated, their spinal cords were flushed out according to a previously published method [28]. Briefly, the spinal column was sectioned at about the 4th sacral vertebra. A 20″–22″ gauge needle attached to a 10 ml syringe was inserted into the caudal opening of the spinal column. Approximately 5 ml of PBS was gently injected to flush the spinal cord from the rostral end of the severed spinal column. The cord was then sectioned into cervical, thoracic, lumbar, and sacral regions according to a template that served as a visual aid (Fig. S1). The template was constructed based on anatomic atlas of the rat spinal cord [29].

Homogenate

All glassware was washed with strong acids (i.e., nitric acid and perchloric acid) to remove possible contamination for trace elements [30] that may interfere fluorometric zinc analysis. The spinal cord sections were weighed and placed in a pre-chilled 1 ml glass homogenizer on ice. Ten volumes of tissue homogenization buffer (0.32 M sucrose; 10 mM HEPES; 0.5 mM $MgSO_4$; 10 mM ε-amino caproic acid; pH 7.4) and the tissues (10 vol. buffer/g wet tissue) were gently homogenized on ice with 10–15 strokes (just enough to completely dissociate the tissue) using the cooled pestle. The protein concentrations were determined by the bicinchoninic acid (BCA) spectrophotometric method (Thermo Scientific, Pierce™ BCA Protein Assay Kit; Cat#23227) and the homogenate aliquots were stored at − 80 °C until use.

Western Blot Analysis

Spinal cord section homogenates were resolved in pre-cast 4–20% SDS/PAGE (Bio-Rad, mini-PROTEAN TGX™ gels; Cat#456–1095) under the reducing conditions. The proteins were transferred onto a transfer membrane (Millipore, Immobilon® PVDF membrane, Cat#IPFL00010) and probed with anti-$Calcineurin_{\alpha}$, (Cat#C1956; Sigma-Aldrich, St Louis, MO, USA; monoclonal antibody) anti-$Calcineurin_{\beta}$, (Cat#C0581; Sigma-Aldrich, St Louis, MO, USA; monoclonal antibody), anti-SOD1 (Cat#100269-1-AP; Protein Tech, USA, Rabbit polyclonal antibody), and anti-TDP-43 (Cat#10782-2-AP; Protein Tech, USA) antibodies. Odyssey/LI-COR detection system (LI-COR Biosciences, Nebraska, USA) was used for analyzing the protein bands (Image Studio Ver.3.1).

Zinc Analysis

Spinal cord tissue homogenates were centrifuged (16 K×*g*; 30 min at 4 °C) in order to obtain a clear supernatant. Protein concentrations were measured by BCA assay. The supernatant samples were prepared for Zn assay analysis and the concentrations were measured by a fluorometric Zinc quantification kit (Abcam Inc., USA; Cat#ab176725) according to the manufacturer's provided protocol. A Bio-Tek

microplate reader (Model: Synergy HT, USA equipped with Gen 5 software version 2.05.5) was used for the fluorescence measurement.

Statistical Analysis

Mann–Whitney U rank sum tests followed by the calculation of two-tailed p values were used for determining the significance between groups. SigmaPlot (ver.12.5) was used for graphing and statistical analysis.

Results

Calcineurin Protein Levels Were Lower in Tg Cervical and Thoracic Regions of the Spinal Cord

We analyzed protein levels of both the catalytic subunit of Calcineurin (Cn_A or PPP3CA) and the regulatory subunit (Cn_B or PPP3R1). We observed significantly lower catalytic subunit protein levels in the cervical ($P \leq 0.001$) and thoracic ($P \leq 0.008$) spinal cord of Tg animals, but not in the lumbar region ($P \leq 0.130$) in (Fig. 1a). There were no differences in the Cn_B-regulatory subunit protein levels between the two groups (Fig. 1b). We were unable to harvest sufficient tissue from the sacral region to perform Cn_A and Cn_B western blot analysis.

TDP-43 Protein Levels in Spinal Cord Regions

We measured spinal cord TDP-43 protein levels by Western blot analysis. We observed an increasing trends of TDP-43 in thoracic, lumbar, and sacral regions; however, no statistically significant differences in TDP-43 between Tg and WT rats in any of the regions measured (Fig. 2).

Predicted Phosphorylation Site Analysis for TDP-43

We have employed a computer based Predictor of Natural Disordered Region (PONDR®) algorithm using TDP-43 sequence (NCBI accession code: Q5R5W2.1). Disordered Enhanced Phosphorylation Predictor (DEPP) analysis predicted 28 potential phosphorylation sites and a majority of them were Ser amino acid enriched on the C-terminus (aa 369–410) (Fig. S5).

Higher Zn Concentrations Were Measured in Tg Lumbar Spinal Cord

We measured the total Zn concentrations in all regions of rat spinal cord (Fig. 3). We measured significantly greater Zn in the lumbar region of Tg animals ($P \leq 0.01$). The greater

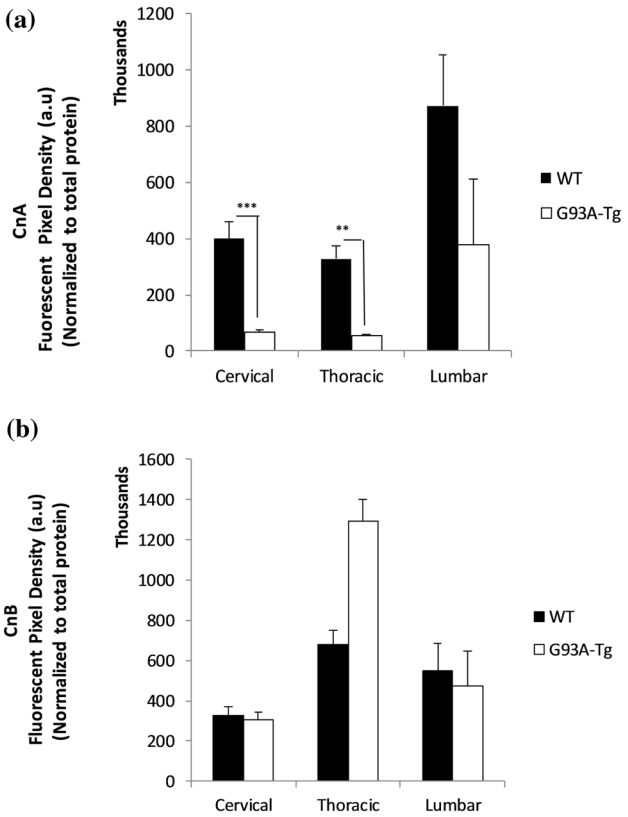

Fig. 1 **a** Catalytic subunit CnA protein levels. Significantly lower catalytic subunit protein levels were observed in the cervical ($P \leq 0.001$) and thoracic ($P \leq 0.008$) spinal cord of Tg animals, but not in the lumbar region ($P \leq 0.130$). Each bar represents the average of five animals for each group ($n = 5$). Data are mean ± SEM. **b** Regulatory subunit CnB protein levels. No differences were observed in the CnB-regulatory subunit protein levels between the two groups. Data are mean ± SEM ($n = 5$)

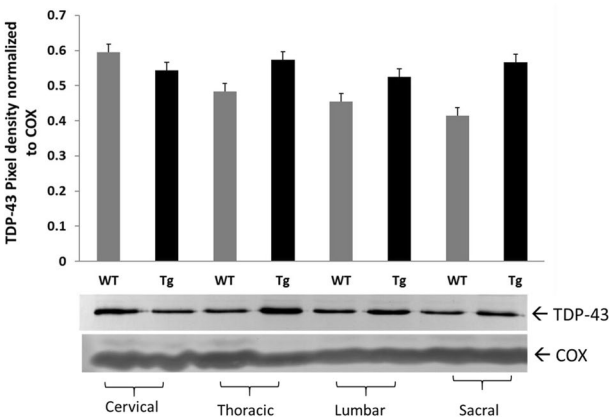

Fig. 2 TDP-43 protein levels in spinal cord regions of SOD1G93A Tg rat. TDP-43 protein levels in spinal cord regions of WT ($n = 6$) and Tg ($n = 8$) animals. Pan anti-TDP-43 Ab was used for Western blot analysis. No statistically significant difference was observed in cervical ($P < 0.0663$), in thoracic ($P < 0.250$), in lumbar ($P < 0.393$), and in sacral ($P < 0.157$) regions of WT and Tg animals. Data are mean ± SEM

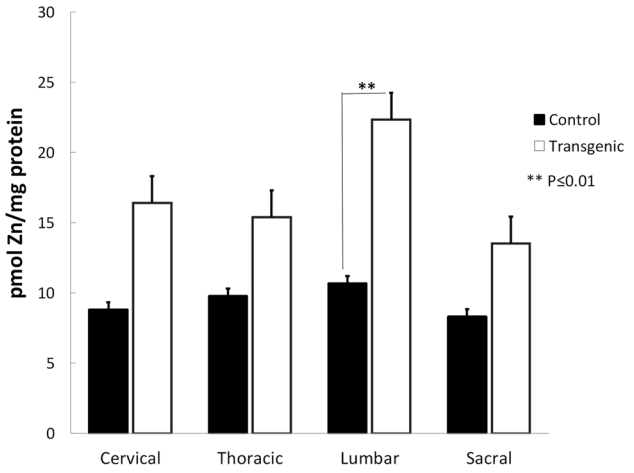

Fig. 3 Zinc concentrations in rat spinal cord regions. Significantly greater Zn concentrations were measured in the lumbar region of Tg animals (**P ≤ 0.01). The Zn levels in the cervical, thoracic, and sacral regions did not reach statistical significance. Data are mean ± SEM (n = 5)

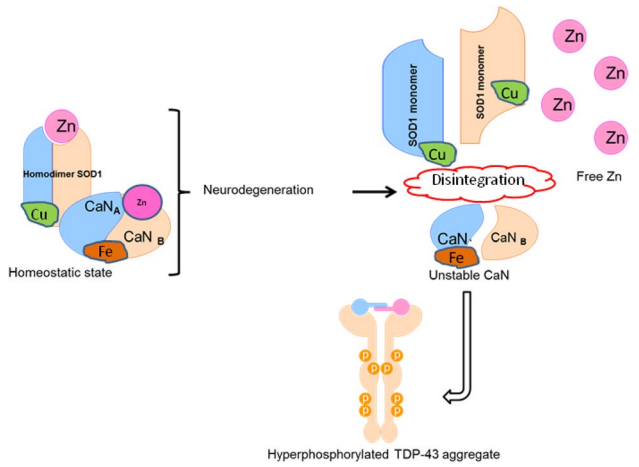

Fig. 4 Proposed model for Cn–SOD1 impaired interaction that leads for TDP-43 aggregation and Zn accumulation in ALS

Zn levels in the cervical, thoracic, and sacral regions did not reach statistical significance.

Discussion

We previously showed that Cn activity depends on the presence of normal homodimer SOD1 in vitro and concluded that Cn–SOD1 interactions actually protect SOD1 dimers from oxidative modification [31]. Evidence provided in the literature suggests that depletion of Zn likely leads the SOD1 protein to undergo aggregation under oxidative conditions [32, 33] We have hypothesized that (1) the mutation in $SOD1^{G93A}$ weakens Zn binding in SOD1 [34]; leading the protein misfolding; (2) this abnormal SOD1 may not efficiently interact with Cn, promoting Zn loss and reduced activity in Cn [31]; (3) less active Cn fails to dephosphorylate TDP-43, leading TDP-43 hyperphosphorylation; (4) failed SOD1–Cn interactions contributes to Zn accumulation. Data provided in this study are in agreement with this hypothesis. We have observed reduced Cn protein amounts in rat spinal cord samples as determined by Western blot analysis (Fig. 1a, b). In unpublished data, we also observed reduced Cn phosphatase activity levels in Tg $SOD1^{G93A}$ mice (Fig. S2). We did not analyze Cn enzyme activity levels in spinal cord homogenates in rat due to insufficient amount of samples; however, we predict that low Cn levels reflect low Cn ativity. We have tested both Cn_A (~61 kDa calmodulin-binding catalytic subunit) and Cn_B (~19 kDa Ca^{2+}/calmodulin-binding regulatory subunit) protein levels in spinal cord regions and found that Cn_A protein level was significantly lower in Tg $SOD1^{G93A}$ rat spinal cord regions as compare to WT (Fig. 1a). On the other hand, Cn_B subunit levels did not differ between the two groups (Fig. 1b). Although we observed a Cn_B upregulation pattern in thoracic region of Tg animals, this increase did not reach statistically significant level. Cn_B subunit is involved in the apoptotic reaction cascade in neurodegeneration [34]. We expected that Cn_B subunit upregulation would be observed in the spinal cord tissue homogenates. Based on these observations, we propose that Cn–SOD1 interaction fails due to alterations in the $SOD1^{G93A}$ mutation, then the less active Cn fails to dephosphorylate TDP-43; consequently, hyperphosphorylated TDP-43 begins to aggregate (Fig. 4). Because the impaired SOD1–Cn interaction is not stabilized, Zn ions would be dissociated from both Cn and SOD1 and form aggregates. The molar ratio between SOD1:Cn was determined to be 2:1 in in vitro conditions for proper Cn activity [31]. Even though $TgSOD1^{G93A}$ rat expresses more SOD1 (Fig. S3), Cn levels remained low in thoracic and lumbar spinal cord regions. Decreased Cn enzyme activity in lymphocytes from ALS patients was also reported in the literature [15].

Recent studies have suggested that Zn dyshomeostasis occurs in spinal cords of $SOD1^{G93A}$ transgenic mice and may contribute to motoneuron degeneration [35, 36]; however, these studies do not specify the region(s) of the spinal cord where Zn accumulation is prevalent. In this study, we found that greater Zn concentration is present in the lumbar spinal cord of $SOD1^{G93A}$ rats (Fig. 3) and mice (Fig. S4).

The labile Zn aggregation in neurons and astrocytes in the spinal cord of $SOD1^{G93A}$ transgenic mice supports the concept of the Zn dyshomeostasis in ALS [22]. Zinc is an essential cofactor for enzymatic activity and 10% of all mammalian proteins require Zn for proper folding [37]. Although Zn modulates the function of many other proteins,

its homeostasis is poorly understood in health and in disease conditions. The elevated toxic levels of trace element Zn were reported in ALS patients reviewed by Smith and Lee [38], suggesting the link between environmental causes and an increased incidence of the disease. A possible approach would be to study the metal binding properties of SOD1, since SOD1 is a metalloprotein and binds to both Cu and Zn. The G93A SOD1 mutation selectively destabilizes the remote metal binding region (i.e., Zn and Cu binding region) [39]. We have proposed a model (Fig. 4) where unstable Zn-deficient SOD1 proteins may destabilize Cn that weakly binds Zn [31], causing impaired SOD1–Cn interaction. Subsequently, destabilized Cn fails to dephosphorylate TDP-43, leading to TDP-43 protein aggregation. However, this model needs to be tested in cell-based studies. Alterations in the metal-binding sites of another mutant $SOD1^{G85R}$ contributes to toxicity in SOD1-linked ALS [40]. This observation further supports the notion that Zn deficiency may contribute to the less stable SOD1 which enhances SOD1 aggregation in neuronal cells. This hypothesis was recently challenged by reports that SOD1 stabilization is not due to dimerization and proper metallation but disulfide formation between two SOD1 homodimer [40, 41]. In addition, liberated Zn may create local metal toxicity. There are extensive reports identifying the neurotoxic effects of Zn, however the mechanism remain unclear [42].

Calcineurin is a Ser/Thr specific phosphatase [16]. Ser amino acid enriched C-terminus region of TDP-43 (Fig. S5) is a potential substrate for Cn. Therefore, decreased activity of Cn may impair the dephosphorylation of TDP-43; hence, TDP-43 aggregations form in $SOD1^{G93A}$ Tg rat spinal cord tissue (Fig. 2, Fig. S6).

In conclusion, the complex biology of ALS necessitates the study of relevant biochemical events so that logical connections among the biomolecules and metal ions can be established. In this study, we have demonstrated that impaired $SOD1^{G93A}$–Cn interaction gave rise to three important consequences in vivo; (1) reduced Cn enzyme levels, (2) labile Zn accumulation, and (3) TDP-43 aggregation. These events would potentially have contributed to ALS progression in the rat model. Further studies should design effective small molecules that maintain Cn activity so that hyperphosphorylated TDP-43 aggregation is controlled if not stopped. Stabilized Cn would not contribute labile Zn after dissociation from Cn molecule; therefore, Zn aggregation would be relatively less.

Acknowledgements We thank Justine Thomas, Megan Liberty, Tess Lamack, Mina Tawadrous, and Prabhal Sandhu for their contributions in experimental phase of this manuscript. Financial support is from KCU intramural grants awarded for AA and from GM103418 to JAS.

Authors' Contributions JMK, EB, AR, TN, JS, EA, MT, and IM performed the experiments, acquired data, and constructed the graphs. EA and JAS critically read the manuscript. JAS provided the rat spinal cord samples and critical reading the manuscript. AA planned and organized the experiments and results, sketched the illustration and wrote the manuscript.

Funding This work was supported by a intramural grant for AA from KCU and Summer Research Fellowship Awards for JMK and EB.

Compliance with Ethical Standards

Conflict of interest The authors declare that they have no conflict of interest.

Informed Consent Informed consent was obtained from all individual participants included in the study.

References

1. Olanow CW (1993) A radical hypothesis for neurodegeneration. Trends Neurosci 16(11):439–444
2. Kato S et al (2004) Histological evidence of redox system breakdown caused by superoxide dismutase 1 (SOD1) aggregation is common to SOD1-mutated motor neurons in humans and animal models. Acta Neuropathol 107(2):149–158
3. Neumann M et al (2006) Ubiquitinated TDP-43 in frontotemporal lobar degeneration and amyotrophic lateral sclerosis. Science 314(5796):130–133
4. Arai T et al (2006) TDP-43 is a component of ubiquitin-positive tau-negative inclusions in frontotemporal lobar degeneration and amyotrophic lateral sclerosis. Biochem Biophys Res Commun 351(3):602–611
5. Chen-Plotkin AS, Lee VM, Trojanowski JQ (2010) TAR DNA-binding protein 43 in neurodegenerative disease. Nat Rev Neurol 6(4):211–220
6. Forman MS, Trojanowski JQ, Lee VM (2007) TDP-43: a novel neurodegenerative proteinopathy. Curr Opin Neurobiol 17(5):548–555
7. Fiesel FC, Kahle PJ (2011) *TDP-43 and FUS/TLS*: cellular functions and implications for neurodegeneration. FEBS J 278(19):3550–3568
8. Ilieva H, Polymenidou M, Cleveland DW (2009) Non-cell autonomous toxicity in neurodegenerative disorders: ALS and beyond. J Cell Biol 187(6):761–772
9. Wegorzewska I, Baloh RH (2011) TDP-43-based animal models of neurodegeneration: new insights into ALS pathology and pathophysiology. Neurodegener Dis 8(4):262–274
10. Liachko NF, Guthrie CR, Kraemer BC (2010) Phosphorylation promotes neurotoxicity in a Caenorhabditis elegans model of TDP-43 proteinopathy. J Neurosci 30(48):16208–16219
11. Chong PA, Forman-Kay JD (2016) A new phase in ALS research. Structure 24(9):1435–1436
12. Neumann M et al (2009) Phosphorylation of S409/410 of TDP-43 is a consistent feature in all sporadic and familial forms of TDP-43 proteinopathies. Acta Neuropathol 117(2):137–149

13. Neumann M et al (2007) TDP-43-positive white matter pathology in frontotemporal lobar degeneration with ubiquitin-positive inclusions. J Neuropathol Exp Neurol 66(3):177–183
14. Liachko NF et al (2016) The phosphatase calcineurin regulates pathological TDP-43 phosphorylation. Acta Neuropathol 132(4):545–561
15. Ferri A et al (2004) Activity of protein phosphatase calcineurin is decreased in sporadic and familial amyotrophic lateral sclerosispatients. J Neurochem 90(5):1237–1242
16. Klee CB, Draetta GF, Hubbard MJ (1988) Calcineurin. Adv Enzymol Relat Areas Mol Biol 61:149–200
17. Rusnak F, Mertz P (2000) Calcineurin: form and function. Physiol Rev 80(4):1483–1521
18. King MM, Huang CY (1984) The calmodulin-dependent activation and deactivation of the phosphoprotein phosphatase, calcineurin, and the effect of nucleotides, pyrophosphate, and divalent metal ions. Identification of calcineurin as a Zn and Fe metalloenzyme. J Biol Chem 259(14):8847–8856
19. Giri PR et al (1992) Molecular and phylogenetic analysis of calmodulin-dependent protein phosphatase (calcineurin) catalytic subunit genes. DNA Cell Biol 11(5):415–424
20. Sirangelo I, Iannuzzi C (2017) The role of metal binding in the amyotrophic lateral sclerosis-related aggregation of copper–zinc superoxide dismutase. Molecules 22(9):1429
21. Mera-Adasme R et al (2016) Destabilization of the metal site as a hub for the pathogenic mechanism of five ALS-linked mutants of copper, zinc superoxide dismutase. Metallomics 8(10):1141–1150
22. Kim J et al (2009) Accumulation of labile zinc in neurons and astrocytes in the spinal cords of G93A SOD-1 transgenic mice. Neurobiol Dis 34(2):221–229
23. Tiwari A, Hayward LJ (2005) Mutant SOD1 instability: implications for toxicity in amyotrophic lateral sclerosis. Neurodegener Dis 2(3–4):115–127
24. Cuajungco MP, Lees GJ (1997) Zinc metabolism in the brain: relevance to human neurodegenerative disorders. Neurobiol Dis 4(3–4):137–169
25. Li C et al (2013) Cupric ions induce the oxidation and trigger the aggregation of human superoxide dismutase 1. PLoS ONE 8(6):e65287
26. Limpert AS, Mattmann ME, Cosford ND (2013) Recent progress in the discovery of small molecules for the treatment of amyotrophic lateral sclerosis (ALS). Beilstein J Org Chem 9:717–732
27. Yao X (2009) Effect of zinc exposure on HNE and GLT-1 in spinal cord culture. Neurotoxicology 30(1):121–126
28. Parone PA, Cruz SD, Cleveland DW (2013) Mitochondrial isolation and purification from mouse spinal cord. Bio Protoc 3(21):e961
29. Sengul G et al (2013) Atlas of the spinal cord. 1st edn. Academic Press, Amsterdam, p 360
30. Alcock NW (1987) A hydrogen-peroxide digestion system for tissue trace-metal analysis. Biol Trace Elem Res 13(1):363–370
31. Agbas A et al (2007) Activation of brain calcineurin (Cn) by Cu–Zn superoxide dismutase (SOD1) depends on direct SOD1-Cn protein interactions occurring in vitro and in vivo. Biochem J 405(1):51–59
32. Rakhit R et al (2007) An immunological epitope selective for pathological monomer-misfolded SOD1 in ALS. Nat Med 13(6):754–759
33. Rakhit R et al (2002) Oxidation-induced misfolding and aggregation of superoxide dismutase and its implications for amyotrophic lateral sclerosis. J Biol Chem 277(49):47551–47556
34. Wu Y, Song W (2013) Regulation of RCAN1 translation and its role in oxidative stress-induced apoptosis. FASEB J 27(1):208–221
35. Trumbull KA, Beckman JS (2009) A role for copper in the toxicity of zinc-deficient superoxide dismutase to motor neurons in amyotrophic lateral sclerosis. Antioxid Redox Signal 11(7):1627–1639
36. Leal SS et al (2015) Aberrant zinc binding to immature conformers of metal-free copper-zinc superoxide dismutase triggers amorphous aggregation. Metallomics 7(2):333–346
37. Cox EH, McLendon GL (2000) Zinc-dependent protein folding. Curr Opin Chem Biol 4(2):162–165
38. Smith AL, Lee NM (2007) Role of zinc in ALS. Amyotroph Lateral Scler 8:131–143
39. Museth AK et al (2009) The ALS-associated mutation G93A in human copper-zinc superoxide dismutase selectively destabilizes the remote metal binding region. Biochemistry 48(37):8817–8829
40. Cao X et al (2008) Structures of the G85R variant of SOD1 in familial amyotrophic lateral sclerosis. J Biol Chem 283(23):16169–16177
41. Chattopadhyay M et al (2015) The disulfide bond, but not zinc or dimerization, controls initiation and seeded growth in amyotrophic lateral sclerosis-linked Cu, Zn superoxide dismutase (SOD1) fibrillation. J Biol Chem 290(51):30624–30636
42. Malaiyandi LM et al (2005) Direct visualization of mitochondrial zinc accumulation reveals uniporter-dependent and -independent transport mechanisms. J Neurochem 93(5):1242–1250